Journal of Geriatric Cardiology JGC
RESEARCH ARTICLE
J Geriatr Cardiol 2021; 18(12): 1029–1043

MiR-21-5p-expressing bone marrow mesenchymal stem cells alleviate myocardial ischemia/reperfusion injury by regulating the circRNA_0031672/miR-21-5p/programmed cell death protein 4 pathway

Jing ZHANG[1], Chang-Jun LUO[1], Xiao-Qi XIONG[1], Jun LI[1], San-Hua TANG[1], Lin SUN[2], Qiang SU[3,✉]

1. Department of Cardiovascular Medicine, Liuzhou Municipal Liutie Central Hospital, Liuzhou, China; 2. Department of Clinical Laboratory, Liuzhou Municipal Liutie Central Hospital, Liuzhou, China; 3. Department of Cardiology, Affiliated Hospital of Guilin Medical University, Guangxi, China
✉ Correspondence to: suqiang1983@foxmail.com
https://doi.org/10.11909/j.issn.1671-5411.2021.12.004

ABSTRACT

BACKGROUND For patients with coronary heart disease, reperfusion treatment strategies are often complicated by ischemia/reperfusion (I/R) injury (IRI), leading to serious organ damage and malfunction. The miR-21/programmed cell death protein 4 (PDCD4) pathway is involved in the IRI of cardiomyocytes; however, the aberrant miR-21 expression remains unexplained. Therefore, this study aimed to explore whether circRNA_0031672 downregulates miR-21-5p expression during I/R and to determine whether miR-21-5p-expressing bone marrow mesenchymal stem cells (BMSCs) reduce myocardial IRI.

METHODS CircRNA_0031672, miR-21-5p, and PDCD4 expressions were evaluated in the I/R rat model and hypoxia/re-oxygenation (H/R)-treated H9C2 cells. Their interactions were subsequently investigated using luciferase reporter and RNA pull-down assays. Methyltransferase-like 3, a methyltransferase catalyzing N6-methyladenosine (m6A), was overexpressed in H9C2 cells to determine whether m6A modification influences miR-21-5p targeting PDCD4. BMSCs stably expressing miR-21 were co-cultured with H9C2 cells to investigate the protective effect of BMSCs on H9C2 cells upon H/R.

RESULTS I/R downregulated miR-21-5p expression and upregulated circRNA_0031672 and PDCD4 expressions. CircRNA_0031672 knockdown increased miR-21-5p expression, but repressed PDCD4 expression, indicating that circRNA_0031672 competitively bound to miR-21-5p and prevented it from targeting PDCD4 mRNA. The m6A modification regulated PDCD4 expression, but had no effect on miR-21-5p targeting PDCD4. The circRNA_0031672/miR-21-5p/PDCD4 axis regulated myocardial cells viability and apoptosis after H/R treatment; co-culture with miR-21-5p-expressing BMSCs restored miR-21-5p abundance in H9C2 cells and further reduced H9C2 cells apoptosis induced by H/R.

CONCLUSIONS We identified a novel circRNA_0031672/miR-21-5p/PDCD4 signaling pathway that mediates the apoptosis of cardiomyocytes and successfully alleviates IRI in myocardial cells by co-culture with miR-21-5p-expressing BMSCs, offering novel insights into the IRI pathogenesis in cardiovascular diseases.

Coronary heart disease (CHD) is a major cause of death globally. According to the data released by the World Health Organization, the mortality rate due to CHD in China is the second highest in the world. Current therapeutic approaches for acute myocardial infarction include reperfusion strategies such as drug thrombolysis, coronary intervention, and vascular bypass grafting.[1] However, the accompanying effect of ischemia/reperfusion (I/R) injury (IRI) remains unsolved. The IRI is a pathophysiologic process which can cause tissue damage and deterioration of multiple organs, ultimately leading to organ malfunction.[2,3] Although multiple proposals have been made regarding the pathogenesis of IRI,[1,4,5] further evidence is needed to understand the precise mechanisms.

Therefore, delineating the detailed mechanisms underlying IRI is of vital importance for realizing the goal of early restoration of blood flow in ischemic tissues with minimal reperfusion injuries.

MicroRNAs (miRNAs), 20–25 nucleotide-long non-coding RNAs, have been extensively studied and reported to modulate multiple cellular processes and cell signaling pathways by regulating the expression of messenger RNAs (mRNAs). MiRNAs also participate in regulating the response of cardiomyocytes to IRI by regulating various genes related to myocardial cell survival and apoptosis.[6–8] Circular RNA (circRNA) is a less studied non-coding RNA. CircRNAs are mainly located in the cytoplasm and contain miRNA response elements that facilitate circRNAs to act as miRNA sponges through competitive interaction and inhibition of miRNA functions.[9] Multiple studies have validated the circRNA-miRNA regulatory machinery and established the role of circRNA as a competing endogenous RNA.[10–12]

Among multiple types of RNA methylation modifications, including N1-methyladenosine, 5-methylcytosine, 5-hydroxymethylcytosine, N6-methyladenosine (m6A), and 7-methylguanine,[13] the m6A modification occurs abundantly in mammals, accounting for almost half of the total RNA methylation events and playing crucial roles in RNA regulation.[14,15] The m6A modification is often enriched near 3′ untranslated region (3′UTR), where miRNA binding sites may be present, raising the possibility of m6A and miRNA cooperatively or competitively targeting mRNAs.[16]

Bone marrow mesenchymal stem cells (BMSCs), the first type of mesenchymal stem cells identified, have attracted substantial attention for their pluripotency and ability to secrete extracellular vesicles. Large quantities of RNA or protein products generated by genetically modified BMSCs can be subsequently secreted extracellularly and internalized by surrounding cells, enabling BMSCs to be applied in clinical settings as potential vectors for gene therapy.[17] In addition, BMSCs are reported to be a promising candidate in alleviating myocardial infarction or even heart failure.[18,19]

Apoptosis plays a major role in IRI and is considered a potential indicator of IRI severity. In particular, miR-21 has been shown to affect the apoptosis of myocardial cells by regulating the expression of multiple target genes.[20,21] Expression of miR-21 has previously been shown to be downregulated in infarcted areas, whereas it is upregulated in the border regions of infarcted areas, and ischemia preconditioning prevented the downregulation of miR-21 in infarcted areas.[22] The anti-apoptotic role of miR-21-5p in myocardial ischemia has been shown to be associated with pathways involving programmed cell death protein 4 (PDCD4) and activated caspase-1.[20]

Our previous study revealed the global alteration of circRNAs in hypoxic cardiomyocytes compared to that in normal controls, while the roles of these circRNAs in cardiomyocyte apoptosis remained elusive. Here, we identified circRNA_0031672, transcribed from the locus of *RALGAPA1*, and found that circRNA_0031672 modulated the apoptosis of cardiomyocytes under hypoxia by acting as a sponge of miR-21-5p. Methyltransferase-like 3 (METTL3), a methyltransferase catalyzing m6A, was overexpressed in H9C2 cells to determine whether the m6A modification influences miR-21-5p targeting PDCD4 mRNA. After confirming that m6A modification had no effect on miR-21-5p targeting PDCD4 mRNA, we co-cultured H9C2 cells with miR-21-5p-expressing BMSCs to reduce H9C2 injury after hypoxia/re-oxygenation (H/R). Thus, we propose a novel molecular mechanism of apoptosis during I/R and provide a potential therapeutic strategy for alleviating IRI in CHD patients by utilizing BMSCs.

MATERIAL AND METHODS

All animal experiments were performed in accordance with guidelines for Animal Research in Liuzhou Municipal Liutie Central Hospital, Liuzhou, China, and the investigation conformed to the guidelines for the Care and Use of Laboratory Animals of National Institutes of Health. The animal study was approved by the Ethics Committee of Liuzhou Municipal Liutie Central Hospital, Liuzhou, China (No. 2018-001-21). The body weight of each Sprague-Dawley rat was recorded before the procedure. Rats were anesthetized with 5% isoflurane in an induction chamber and received a subcutaneous injection of buprenorphine (0.003 mg/mL per 100 g body weight). After the chest wall was opened and the pericardium was removed, coronary ischemia was

induced by ligating the left anterior descending branch of the left coronary artery (1–3 mm from the tip of the normally positioned left auricle) using 6–0 silk suture with a tapered needle. Ischemia was maintained for 45 min, and subsequently, the suture was released to allow reperfusion for 24 h.

Electrocardiogram and Blood Pressure Measurement

Electrocardiogram signals and blood pressure of IRI or the Sham control rats were recorded using a Powerlab biological signal processing system (AD Instruments, Bella Vista, Australia) following the manufacturer's instructions.

Cell Culture and H/R Treatment

H9C2 is a cell line derived from rat embryonic cardiomyoblasts. We purchased H9C2 from the American Type Culture Collection (Rockville, Maryland, USA). BMSCs were obtained from Shanghai Zhongqiao Xinzhou Biotechnology Co., Ltd. (Shanghai, China). These cell lines were cultured at 37 °C in Roswell Park Memorial Institute 1640 medium or Dulbecco's modified Eagle's medium supplemented with 10% fetal bovine serum in a humidified incubator and 5% CO_2. For H/R treatment, H9C2 cells were cultured at 37 °C in an incubator with 5% CO_2, 1% O_2, and 94% N_2 for 12 h and then returned to normal condition for 0–48 h.

Cell Transfection

Small interfering RNA (siRNA)-circRNA_0031672, miR-21-5p mimic, miR-21-5p inhibitor, and siRNA-PDCD4 were constructed at Gemma Gene Co., Ltd. (Shanghai, China). The sequences of these vectors are listed in Table 1. H9C2 cells were transfected using Lipofectamine™ 2000 (Invitrogen Life Technologies, Thermo Fisher, USA) in Opti-MEM medium following the manufacturer's instructions. To overexpress METTL3, cells were transfected with the METTL3 expression vector (pEGFP-C1; Invitrogen Life Technologies, Thermo Fisher, USA), using Lipofectamine™ 2000 (Invitrogen Life Technologies, Thermo Fisher, USA), following the manufacturer's protocol.

Before transfection, 1×10^6 BMSCs were inoculated in 10 mL of MesenCult™-ACF medium and cultured overnight. BMSCs were transfected with the miR-21 lentiviral overexpression vector (Multiplicity of infection = 10.0, Gemma Gene). After 24 h of transfection, BMSCs were collected for quantitative real-time polymerase chain reaction (qRT-PCR) analysis.

qRT-PCR

Total RNA was extracted from cells subjected to different treatments using the Trizol reagent (Invitrogen Inc., Carlsbad, USA). Chloroform was added to the Trizol lysates for RNA extraction. The upper phase was collected, and isopropanol was used to precipitate RNA. The precipitate was washed with 75% ethanol. The obtained RNA (1 μg) was reverse transcribed as a template for real-time PCR amplification using a First-Strand cDNA Synthesis kit (Fermentas, Vilnius, Lithuania). The qRT-PCR was performed using the 7300 Sequence Detection System (Applied Biosystems, Foster City, California, USA) and a SYBR® Green PCR kit (Applied Biosystems, Foster City, California, USA). The PCR primers

Table 1 The sequences of vectors for cell transfection.

Names	Number	Sequences (5′-3′)
SiRNA-circRNA_0031672	1	ATGGACAAGAGGGGAACAGAT
	2	**GACAAGAGGGGAACAGATGCT**
	3	AGAGGGGAACAGATGCTGCTT
MiR-21-5p mimic	1	**UAGCUUAUCAGACUGAUGUUGA**
MiR-21-5p inhibitor	1	**UCAACAUCAGUCUGAUAAGCUA**
SiRNA-PDCD4	1	GTTAATCCACTTCTAAGGGCG
	2	**AAATGTCAGAAATGCCTTGTA**
	3	TAATGTCCGGAATTTCATTGT

The sequences marked in bold were used in the formal experiments. circRNA: circular RNA; PDCD4: programmed cell death protein 4; siRNA: small interfering RNA.

used are listed in Table 2. U6 small nuclear RNA and beta-actin were used as internal controls to calculate the relative expression levels of miRNAs and mRNAs, respectively.

Western Blot

Cells and tissues were solubilized in lysis buffer (No.20-188; Sigma-Aldrich), and the solution was boiled for 5–10 min. Proper amounts of proteins were loaded for sodium dodecyl sulfate-polyacrylamide gel electrophoresis (Sangon Biotech, Shanghai, China) and subsequently transferred onto a polyvinylidene fluoride membrane (Merck Millipore, Germany). The membrane was then blocked with 5% nonfat milk (Sangon Biotech, Shanghai, China) for 2 h at 4 °C, followed by overnight incubation at 4 °C with primary antibodies against PDCD4 (1:250 dilution, Santa Cruz Biotechnology Inc., Santa Cruz, California, USA) and beta-actin (1:1,000 dilution, Santa Cruz Biotechnology Inc., Santa Cruz, California, USA) and peroxidase-conjugated anti-mouse immunoglobulin secondary antibody (Santa Cruz Biotechnology Inc., Santa Cruz, California, USA) at room temperature for 2 h before adding chemiluminescent substrates.

Cell Counting Kit-8 Assay

Cell viability was evaluated using the cell counting kit-8 (Cat. No.HY-K0301, MedChemExpress, Shanghai, China) following the manufacturer's instructions. The cells were seeded in a 96-well plate and subjected to the corresponding treatment after attachment; a total of 10 μL cell counting kit-8 solution was added to each well and incubated for 1 h in the cell incubator before optical density values were determined using a microplate reader at 50 nm.

Flow Cytometry

Annexin V-FITC staining kit (Cat. No.556570, BD Biosciences, USA) was used to determine apoptosis of cells subjected to different treatments. The cells were washed with phosphate-buffered saline, incubated with 500 μL of binding buffer containing 5 μL of Annexin V and 5 μL of propidium iodide for 5 min at room temperature in the dark, and analyzed using a flow cytometer (Becton Dickinson, San Jose, California, USA). Data were analyzed using the ModFit LT™ software (Verity Software House, Topsham, Maine, USA).

Luciferase Assay

Luciferase assays were performed using a luciferase assay kit (Cat. No.BC2500L, Thermo Fisher, USA) following the manufacturer's instructions. The pGL3 reporter plasmids containing PDCD4 3′ UTR sequences of 5′-UCUAAUAAGCUACCUUUU-3′ (wild-type) or 5′-UCUAACAGGUAACCUUUU-3′ (mutant-type) were constructed. The reporter vectors were transfected alone or co-transfected with the miR-21-5p mimic into H9C2 cells. Cells were then harvested and lysed to detect luciferase reporter activity 24 h after transfection. Luciferase activity

Table 2 The primer sequences.

RNA names	Direction	Sequence
CircRNA_0031672	Forward	5′-TTCAAGGGAGAATCAGGCTG-3′
	Reverse	5′-GCTTTTCTACAGTTCCAAGG-3′
PDCD4	Forward	5′-GGGAGTGACGCCCTTAGAAG-3′
	Reverse	5′-ACCTTTCTTTGGTAGTCCCCTT-3′
MiR-21-5p	Forward	5′-CTTACTTCTCTGTGTGATTTCTGTG-3′
	Reverse	5′-ACAACCTTTCCAAAATCCATGAGGC-3′
Methyltransferase-like 3	Forward	5′-TTGTCTCCAACCTTCCGTAGT-3′
	Reverse	5′-CCAGATCAGAGAGGTGGTGTAG-3′
Beta-actin	Forward	5′-CATGTACGTTGCTATCCAGGC-3′
	Reverse	5′-CTCCTTAATGTCACGCACGAT-3′
U6 small nuclear RNA	Forward	5′-CTCGCTTCGGCAGCACA-3′
	Reverse	5′-AACGCTTCACGAATTTGCGT-3′

circRNA: circular RNA; PDCD4: programmed cell death protein 4.

was reported as the average fold change relative to the basal activity of each vector. The luciferase signal intensity was detected using a ChemiDoc MP Imaging System (Bio-Rad, California, USA) station and reported as normalized with respect to the internal reference.

Fluorescence in Situ Hybridization

The fluorescence in situ hybridization analysis was performed using a FISH Tag RNA Multicolor kit (Cat. No.BC2500L, Invitrogen, California, USA) following the manufacturer's instructions, fixed cells were washed with phosphate-buffered saline, blocked, and washed with 70%, 90%, and 100% ethanol. The probe targeting miR-21-5p was added and heated at 94 °C for 2 min, and then hybridized at 42 °C overnight. Images were acquired and recorded using a fluorescence microscope (Olympus, Japan).

RNA Pulldown Assay

RNA extracts were obtained from H9C2 cells, mixed with the denatured RNA of biotinylated wild-type or mutant-type miR-21-5p, and incubated at 4 °C overnight with pre-blocked streptavidin beads (Invitrogen, California, USA). Beads were collected by centrifugation at 20,000 × g for 1 min at 4 °C, and circRNA_0031672 and PDCD4 mRNA were quantified by PCR.

RNA Immunoprecipitation Assay

The RNA immunoprecipitation assay was performed according to the manufacturer's protocol using the EZ-Magna RIP™ RNA-Binding Protein Immunoprecipitation kit (Cat. No.17-701, Millipore, USA). Cell lysates from different groups were incubated with anti-m6A antibody, anti-Ago2 antibody, or immunoglobulin coupled to magnetic beads at 4 °C overnight. The magnetic beads were then washed five times and incubated with proteinase K to digest the associated proteins at 55 °C for 30 min. RNA from the precipitated complex was then extracted and purified for qRT-PCR analysis.

Statistical Analysis

The results were displayed as mean ± SD of three independent experiments. One-way analysis of variance with post-hoc testing was used for multiple comparisons between each group. Paired or unpaired two-tailed Student's *t*-test was used to compare the IRI group and Sham control group. Values of *P*-value < 0.05, 0.01, and 0.001 were considered statistically significant, respectively. Statistical analysis was performed using SPSS 13.0 (SPSS Inc., IBM, Chicago, IL, USA).

RESULTS

CircRNA_0031672, MiR-21-5p, and PDCD4 Expression was Dysregulated After IRI

We initially constructed an animal model of IRI in rats to analyze the molecular changes in cardiomyocytes during I/R (Figure 1A). IRI rat model was generated by ligating the left anterior descending artery for 45 min and reperfusion for 24 h. Electrocardiogram and blood pressure were recorded in the rats of the IRI and Sham control groups (Figure 1B), verifying the generation of a successful IRI model.

As indicated by the results of our previous study, circRNA_0031672 transcribed from *RALGAPA1* was upregulated upon IRI and was related to apoptotic pathways. Based on analysis of the relevant databases, circRNA_0031672 was predicted to contain competitive binding sites for miR-21-5p. Considering that miR-21-5p contains multiple miRNA response elements of PDCD4, a crucial factor mediating the anti-apoptotic role of miR-21 in hypoxia-induced IRI,[23] the relationship between circRNA_0031672, miR-21-5p, and PDCD4 aroused our interest. Therefore, taking advantage of the IRI rat model, as shown in Figure 1, we detected the expression levels of circRNA_0031672, miR-21-5p, and PDCD4 mRNA using PCR in isolated myocardial tissues, showing that circRNA_0031672 and PDCD4 expression was upregulated, whereas miR-21-5p expression was downregulated after IRI (Figure 2A). Protein levels of PDCD4 were subsequently determined, validating the elevated expression levels of PDCD4 during I/R (Figure 2B). RNA levels of circRNA_0031672, miR-21-5p, and PDCD4 and protein levels of PDCD4 were further evaluated in H9C2 cells subjected to H/R treatment, demonstrating that H/R treatment induced the expression of PDCD4 and circRNA_0031672 and suppressed the expression of miR-21-5p, which is consistent with results obtained from IRI rat models (Figure 2C & 2D).

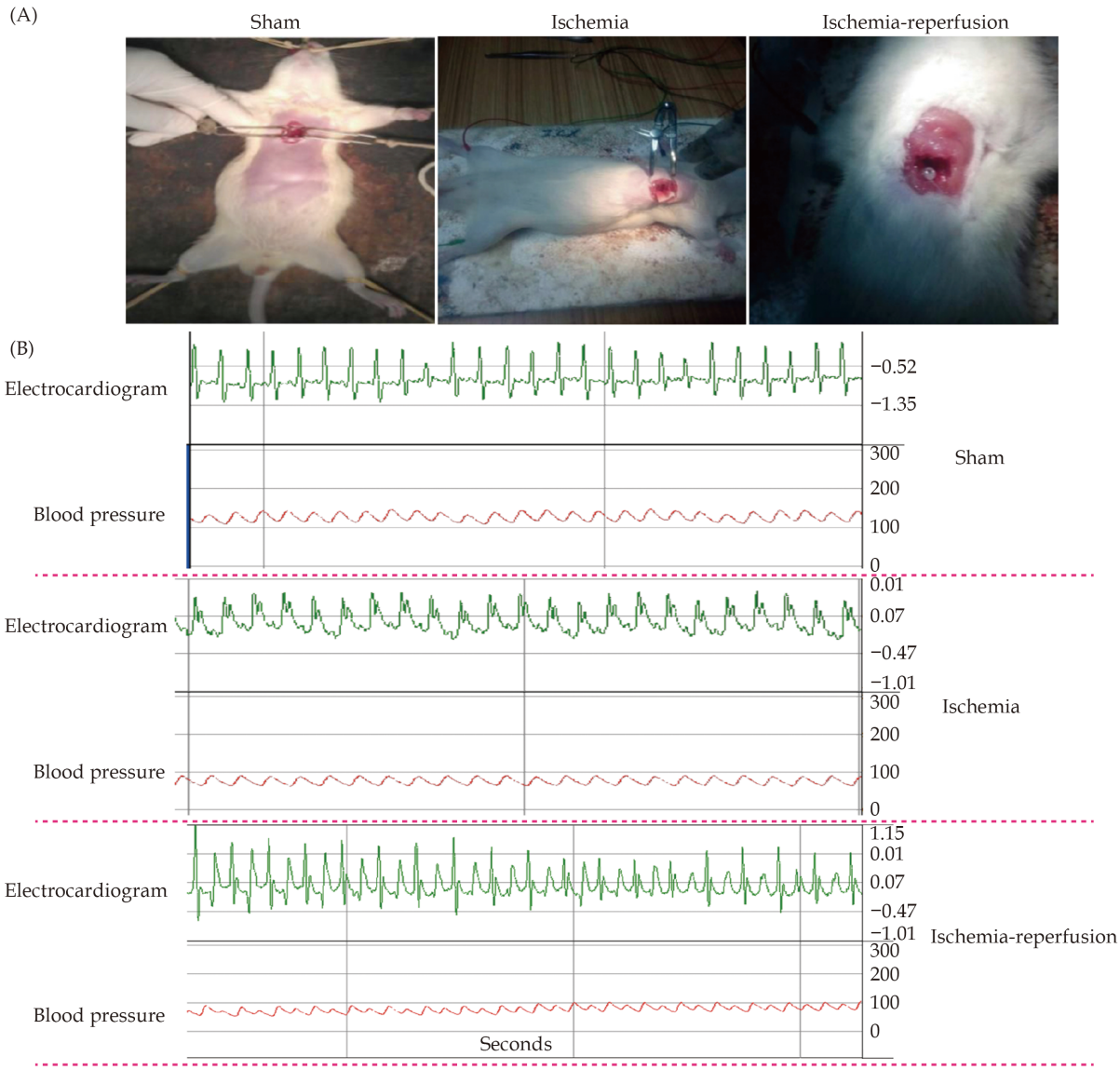

Figure 1 Construction of heart IRI rat models. (A): Illustration of the process of artery ligation and reperfusion or Sham operation in corresponding rats; and (B): demonstration of electrocardiogram and blood pressure of the heart IRI rat models and Sham controls. IRI: ischemia/reperfusion injury.

MiR-21-5p Repressed Expression of CircRNA_0031672 and PDCD4 via Direct Interaction

To further characterize the regulatory mechanisms of circRNA_0031672 and miR-21-5p on PDCD4, we knocked down circRNA_0031672 or RALGAPA1 in H9C2 cells via siRNA transfection. As shown in Figure 3A & 3B, all siRNAs demonstrated proper selectivity for knocking down either circRNA_0031672 or RALGAPA1; the second siRNA for circRNA_0031672 and the first siRNA for RALGAPA1 that illustrated the most prominent impact were selected for further experiments. Knockdown (KD) of circRNA_0031672 enhanced the expression of miR-21-5p and suppressed the expression of PDCD4 (Figure 3C), whereas KD of RALGAPA1 showed no significant effect on the expression of miR-21-5p or PDCD4 (data not shown). We subsequently evaluated the impact of miR-21-5p on PDCD4 expression by transfecting miR-21-5p mimic or inhibitor, with the corresponding results showing that the miR-21-5p inhibitor enhanced the expression of circRNA_0031672 and PDCD4, whereas the miR-21-5p mimic suppressed the expression of circRNA_0031672 and PDCD4 (Figure 3D). Collectively, these results indicate that circRNA_

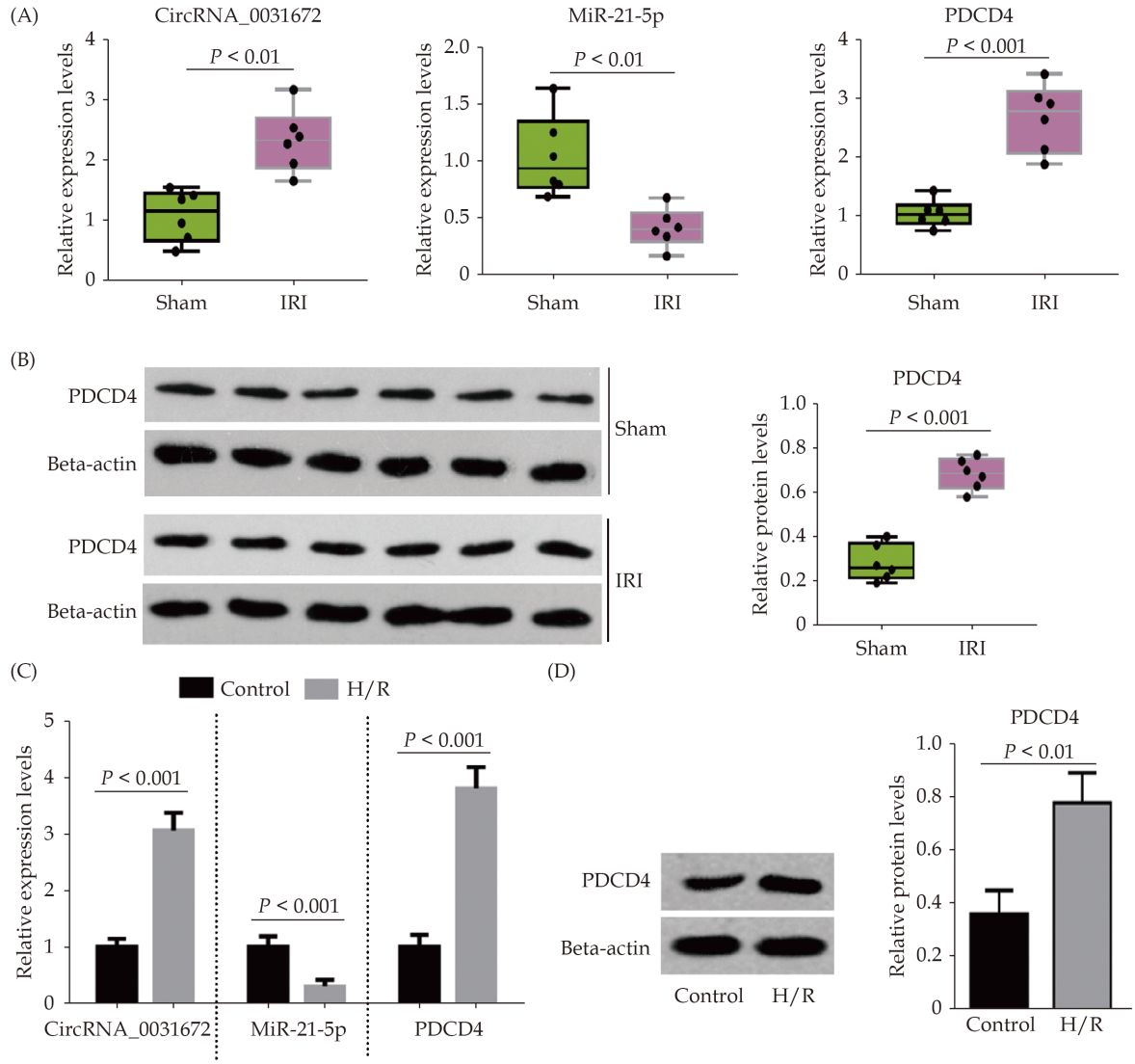

Figure 2 Expression levels of circRNA_0031672, miR-21-5p and PDCD4 in heart IRI rats and H/R treated H9C2 cells. (A): RNA expression levels of circRNA_0031672, miR-21-5p and PDCD4 in myocardial tissues of IRI rats and Sham controls were detected by polymerase chain reaction; (B): protein level of PDCD4 in myocardial tissues of IRI rats and Sham controls was detected by western blot (n = 6); (C): RNA expression levels of circRNA_0031672, miR-21-5p and PDCD4 in H/R-treated H9C2 cells compared to controls were detected by polymerase chain reaction; and (D): protein level of PDCD4 in H/R-treated H9C2 cells compared to controls was detected by western blot (n = 3). circRNA: circular RNA; H/R: hypoxia/re-oxygenation; IRI: ischemia/reperfusion injury; PDCD4: programmed cell death protein 4.

0031672 positively modulates the expression of PDCD4 and that this process may be negatively regulated by miR-21-5p.

Bioinformatic approaches (http://www.targetscan.org/vert_72/) were used to predict the binding sites of circRNA_0031672, miR-21-5p, and PDCD4. Moreover, the target site of miR-21-5p in the 3'UTR of PDCD4 was shown to be conserved among species. The interaction between miR-21-5p and circRNA_0031672 or PDCD4 was then validated using RNA pulldown assays (Figure 3E, column 2 *vs.* column 1). The miR-21-5p mutant-type with a disrupted binding region sequence showed little affinity for circRNA_0031672 or PDCD4 (Figure 3E, column 3 *vs.* column 2) as compared to wild-type miR-21-5p, thus confirming the predicted binding sites among these molecules. PDCD4 wild-type or PDCD4 mutant-type with mutated binding sites was then subjected to a luciferase assay to clarify whether PDCD4 is a downstream target of miR-21-5p.

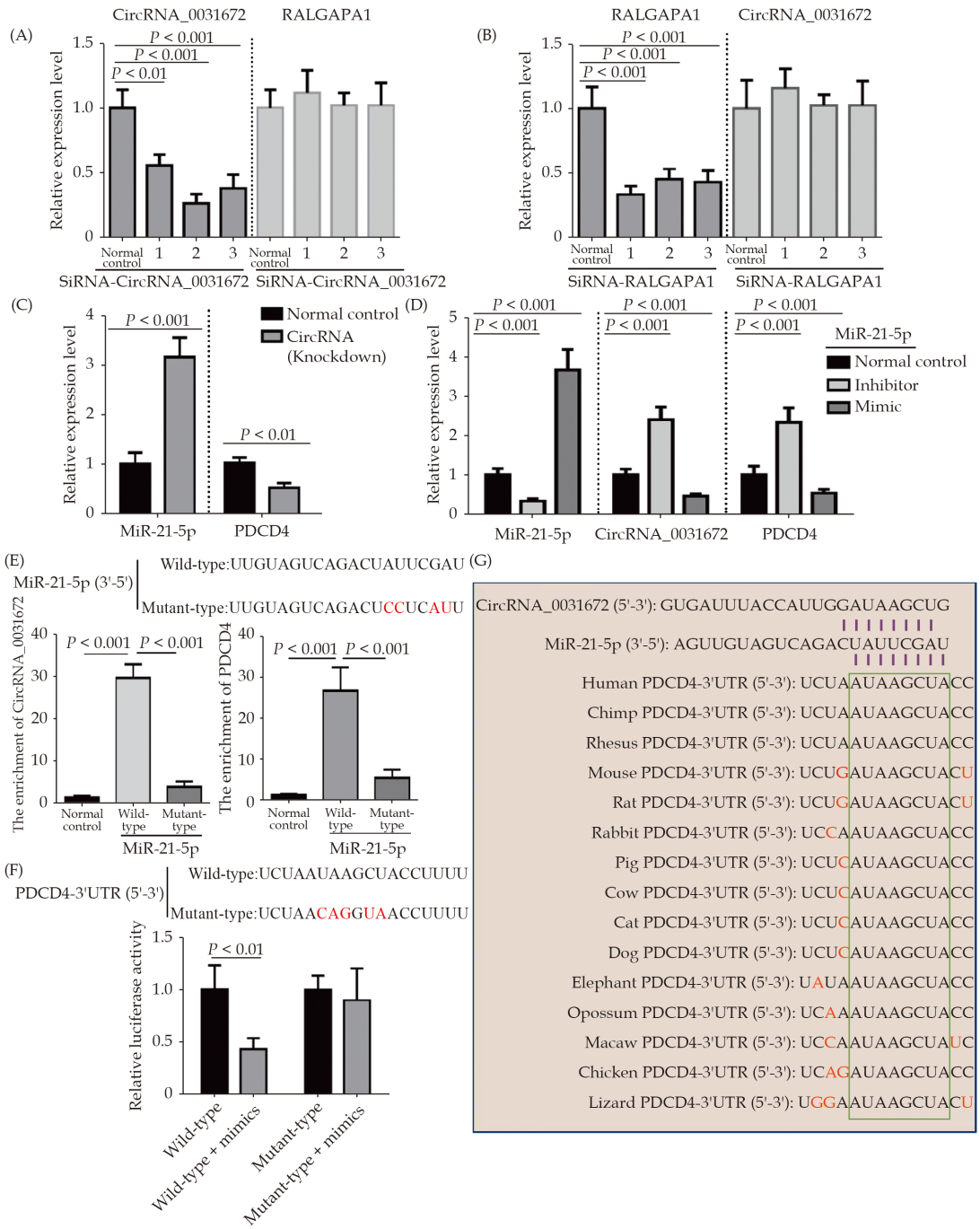

Figure 3 MiR-21-5p directly interacted with circRNA_0031672 and PDCD4 mRNA to regulate their expression. (A): Evaluation of knockdown efficiency of three siRNAs targeting circRNA_0031672 compared to normal control; (B): evaluation of knockdown efficiency of three siRNAs targeting RALGAPA1 compared to normal control; (C): analysis of RNA levels of miR-21-5p and PDCD4 in H92C cells with knockdown of circRNA_0031672 compared to normal control; (D): analysis of RNA levels of circRNA_0031672, miR-21-5p and PDCD4 in H92C cells transfected with miR-21-5p inhibitor, mimic or normal control; (E): analysis of levels of circRNA_0031672 and PDCD4 mRNA enriched by negative control, miR-21-5p wild-type or mutant-type. Altered nucleotides in miR-21-5p mutant-type are marked in red in the upper panel; (F): evaluation of luciferase activities of PDCD4 wild-type or mimic transfected with miR-21-5p mimic or not. Altered nucleotides in 3'UTR of PDCD4 are marked in red in the upper panel; and (G): illustration of binding sites of miR-21-5p in circRNA_0031672 and PDCD4 mRNA. circRNA: circular RNA; mRNA: messenger RNA; PDCD4: programmed cell death protein 4; siRNA: small interfering RNA; 3'UTR: 3' untranslated region.

The results demonstrated that miR-21-5p mimics suppressed the expression level of PDCD4 wild-type instead of PDCD4 mutant-type (Figure 3F), indicating that PDCD4 was directly regulated by miR-21-5p via the predicted binding region. As shown in Figure 3G, a strong binding ability among circRNA_0031672, miR-21-5p, and PDCD4 mRNA is predicted by bioinformatic approaches.

M6A Modification in PDCD4 3'UTR Illustrated no Effect on Interaction with MiR-21-5p

M6A, the most prevalent RNA modification in eukaryotic cells, has been reported to play multiple roles in the regulation of RNA metabolism, including RNA splicing, processing, and RNA decay.[24,25] Considering that adenine exists in the binding region of miR-21-5p in the 3'UTR of PDCD4 mRNA, we wondered whether the m6A modification in the PDCD4 3'UTR affected its interaction with miR-21-5p. Bioinformatics analysis (http://rmvar.renlab.org/) revealed the confidence of all types of modifications in PDCD4 mRNA (Figure 4A). Among these modifications, m6A modification only has medium or low confidence in the PDCD4 mRNA (Figure 4B). By contrast, multiple miRNA regulatory sites existed in the mRNA of PDCD4, suggesting that it was mainly regulated by miRNAs, rather than m6A modifications (Figure 4C). We then analyzed the proteins that interacted with PDCD4 mRNA (Figure 4D). Among the identified proteins, IGF2BP2 and IGF2BP3 were capable of recognizing m6A sites to promote RNA stability and protect RNA from degradation, thereby working against miRNA.

METTL3, a critical subunit of the methyltransferase complex catalyzing m6A modification recognized as an m6A writer,[26] was then used to induce the m6A modification of PDCD4 mRNA. After verifying the successful overexpression (OE) of METTL3 in H9C2 cells transfected with METTL3 (Figure 4E), specific antibodies of m6A were used in the radioimmunoprecipitation assay. The results showed that METTL3 OE significantly elevated the m6A modification levels of PDCD4 mRNA (Figure 4F). Even though m6A in PDCD4 mRNA due to METTL3 OE was elevated, the mRNA levels of PDCD4 were still affected by transfection of miR-21-5p with a mimic or inhibitor (Figure 4G). An RNA pulldown assay demonstrated no obvious variation in the interaction between miR-21-5p and PDCD4 mRNA (Figure 4H), indicating that enhanced m6A in PDCD4 mRNA had no effect on the interaction with miR-21-5p. We subsequently performed radioimmunoprecipitation using an antibody against Ago2, a central component of the gene-silencing complex that mediates mRNA degradation and represses protein translation.[27] The OE of METTL3 resulted in a decrease in Ago2-enriched PDCD4 mRNA, implying that increased m6A modification induced by OE of METTL3 may suppress the degradation of PDCD4 mRNA (Figure 4I, column 2 *vs.* column 1). In addition, the miR-21-5p mimic increased Ago2-enriched PDCD4 mRNA and reversed METTL3-prevented degradation of PDCD4 mRNA (Figure 4I, column 3 & 4 *vs.* column 2), indicating that miR-21-5p promoted the degradation of PDCD4 mRNA via the Ago2 silencing complex. Together, these data suggest that m6A modification of PDCD4 has no impact on its interaction with miR-21-5p.

CircRNA_0031672, MiR-21-5p, and PDCD4 Regulated the Viability and Apoptosis of Cardiomyocytes after H/R Treatment

Our results showed that cells subjected to H/R treatment exhibited reduced cell viability (Figure 5A) and increased apoptosis (Figure 5C), which is consistent with the results of previous studies. The OE of miR-21-5p mimic or KD of PDCD4 or circRNA_0031672 rescued altered cell viability and apoptosis driven by H/R treatment, while OE of miR-21-5p inhibitor enhanced H/R-induced apoptosis (Figure 5A–5C). Furthermore, miR-21-5p inhibitor abolished the protective effect of circRNA_0031672 KD on cell survival, and PDCD4 KD alleviated the pro-apoptotic effect of miR-21-5p inhibitor, implying that circRNA_0031672 acts as an upstream regulator of miR-21-5p, whereas PDCD4 acts as a downstream target of circRNA_0031672 and miR-21-5p in the regulation of myocardial apoptosis (Figure 5A–5C). These data support the conclusion that circRNA_0031672 and miR-21-5p act as upstream regulators of PDCD4, exhibiting the prominent effects of circRNA_0031672/miR-21-5p/PDCD4 axis on cell viability and apoptosis of cardiomyocytes.

Co-culture with BMSCs Stably Expressing MiR-21-5p Rescued Changes in Cardiomyocytes Driven by H/R Treatment

Considering that miR-21-5p is a crucial factor me-

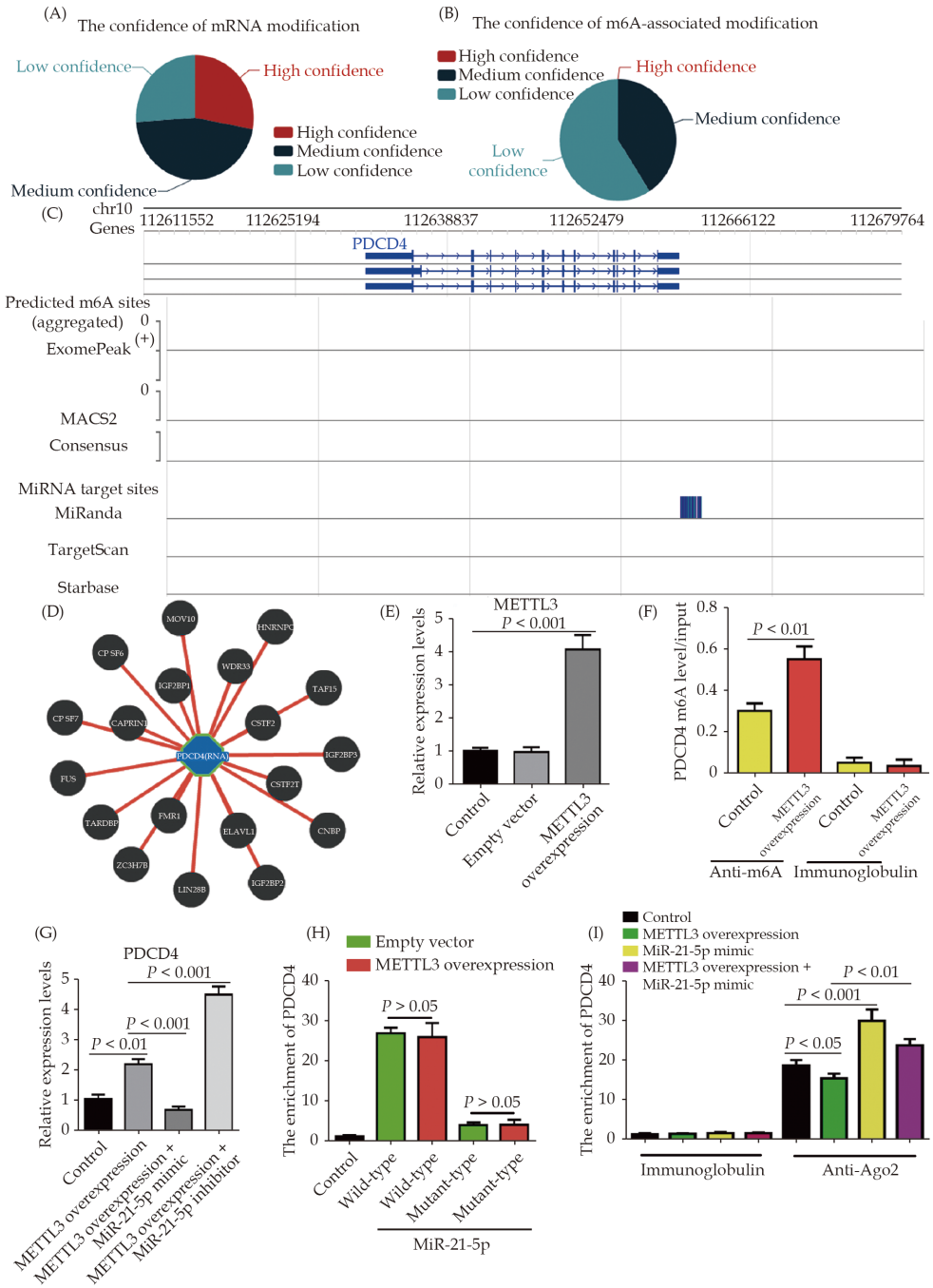

Figure 4 M6A modification in PDCD4 3′ untranslated region showed no effect on miR-21-5p targeting PDCD4 mRNA. (A): Bioinformatic analysis of the confidence of PDCD4 mRNA modification; (B): bioinformatic analysis of the confidence of m6A modification in PDCD4 mRNA; (C): the prediction of m6A regulatory sites and microRNA-targeting sites in PDCD4 mRNA; (D): the prediction of RNA-bind proteins interacting with PDCD4 mRNA; (E): METTL3 expression levels in H9C2 cells transfected with empty vector or vectors for METTL3 overexpression was detected by polymerase chain reaction; (F): the levels of m6A-modified PDCD4 mRNA immunoprecipitated by anti-m6A or immunoglobulin in H9C2 cells transfected with METTL3 or not; (G): polymerase chain reaction analysis of PDCD4 mRNA level in METTL3-overexpressing H9C2 cells co-transfected with miR-21-5p inhibitor or mimic; (H): analysis of PDCD4 mRNA level pulled down by miR-21-5p wild-type or mutant-type in H9C2 cells with METTL3 overexpression or not; and (I): RNA immunoprecipitation analysis of PDCD4 mRNA levels in immunocoprecipitate of anti-Ago2 or immunoglobulin in H9C2 cells transfected with METTL3 overexpression vector, miR-21-5p mimic or both. METTL3: methyltransferase-like 3; mRNA: messenger RNA; m6A: N6-methyladenosine; PDCD4: programmed cell death protein 4.

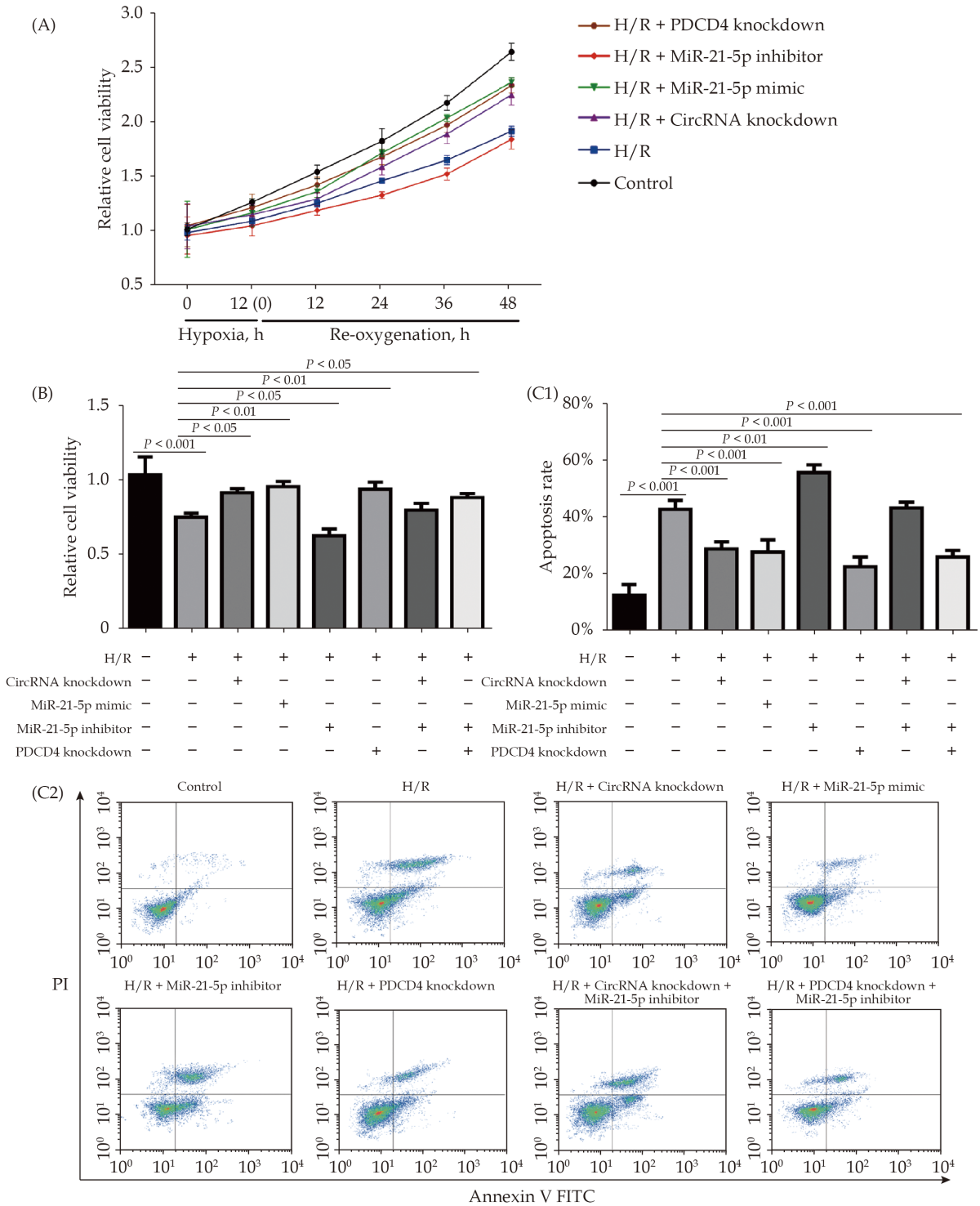

Figure 5 Effects of circRNA_0031672, miR-21-5p and PDCD4 on the viability and apoptosis of H9C2 cells. (A): Time-lapse evaluation of viability of H9C2 cells subjected to hypoxia for 12 h and re-oxygenation for 12–48 h after transfected with corresponding vectors; (B): statistical analysis of viability of H/R-treated H9C2 cells after transfected with corresponding vectors; and (C1 & C2): flow cytometry analysis of apoptosis rate of H/R-treated H9C2 cells after transfected with corresponding vectors. circRNA: circular RNA; H/R: hypoxia/re-oxygenation; PDCD4: programmed cell death protein 4.

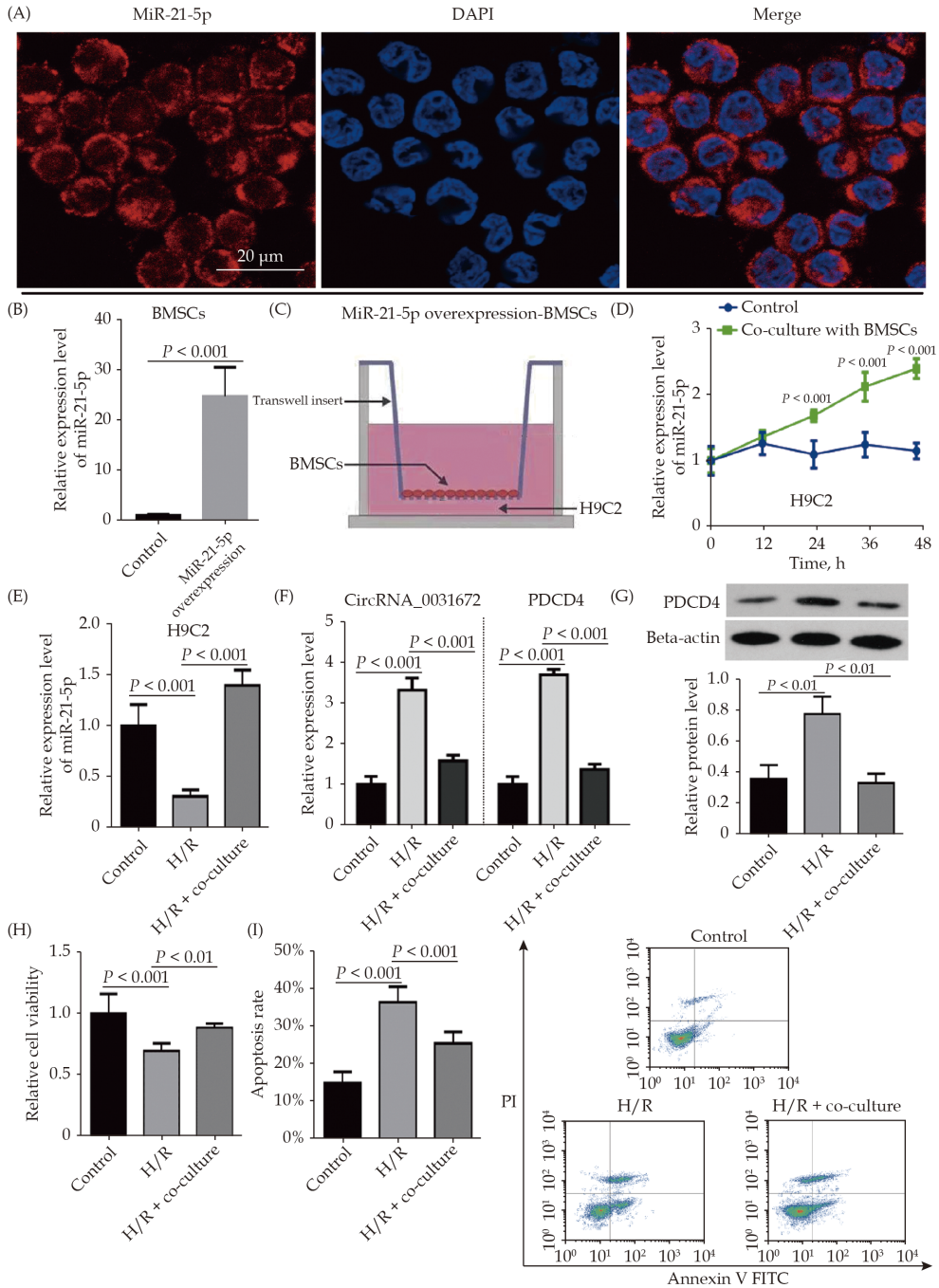

Figure 6 Molecular changes and alteration in cell viability and apoptosis in H/R-treated H9C2 cells co-cultured with miR-21-5p-expressing BMSCs. (A): Validation of miR-21-5p expression in miR-21-5p-expressing BMSCs by fluorescent labeling (red) via a FISH assay. Nuclei were counterstained with DAPI (blue); (B): detection of miR-21-5p levels in miR-21-5p-expressing BMSCs by PCR; (C): graphic illustration of the strategy of co-culturing H9C2 cells with miR-21-5p-expressing BMSCs by a trans-well plate; (D): time-lapse evaluation of miR-21-5p level by PCR in H9C2 cells co-cultured with miR-21-5p-expressing BMSCs or not; (E): evaluation of miR-21-5p level by PCR in H/R-treated H9C2 cells co-cultured with miR-21-5p-expressing BMSCs; (F): evaluation of circRNA_0031672 and PDCD4 mRNA levels by PCR in H/R-treated H9C2 cells co-cultured with miR-21-5p-expressing BMSCs; (G): analysis of PDCD4 by western blotting in H/R-treated H9C2 cells co-cultured with miR-21-5p-expressing BMSCs; (H): analysis of cell viability in H/R-treated H9C2 cells co-cultured with miR-21-5p-expressing BMSCs; and (I): analysis of apoptosis rate in H/R-treated H9C2 cells co-cultured with miR-21-5p-expressing BMSCs. BMSCs: bone marrow mesenchymal stem cells; DAPI: 4′,6-diamidino-2-phenylindole; H/R: hypoxia/re-oxygenation; PCR: polymerase chain reaction.

diating apoptosis of cardiomyocytes, we sought to develop an approach to elevate the intracellular levels of miR-21-5p in cardiomyocytes. BMSCs are characterized by continuous division and multi-vesicle secretion; therefore, we constructed a BMSC line stably expressing miR-21-5p to enable the generation and secretion of miR-21-5p into the extracellular space. As shown by fluorescent labeling in Figure 6A and PCR results in Figure 6B, the miR-21-5p-expressing BMSCs showed a stable expression of miR-21-5p. To investigate whether the BMSCs could efficiently transfer miR-21-5p to cardiomyocytes, we co-cultured BMSCs and H9C2 cells in a transwell plate (Figure 6C). The levels of miR-21-5p in H9C2 were elevated as the time of co-culture increased (Figure 6D). H9C2 cells subjected to H/R treatment showed decreased levels of miR-21-5p, and co-culturing with BMSCs rescued the miR-21-5p levels (Figure 6E). As expected, circRNA _ 0031672 and PDCD4 mRNA demonstrated the opposite trend when subjected to H/R treatment and co-culture with BMSCs (Figure 6F). The protein level and the mRNA expression level of PDCD4 in H9C2 decreased after the co-culture (Figure 6G). Lastly, the effect of co-culturing with BMSCs on cell viability and apoptosis was determined, and the results showed that co-culturing with miRNA-expressing BMSCs rescued H/R-induced cell damage (Figure 6H & 6I).

DISCUSSION

The "dark matter" of the genome was often neglected as it was incapable of coding proteins; however, non-coding RNAs have become a topic of interest in recent years. Non-coding RNAs include miRNA, long non-coding RNA, and circRNA. Among them, miRNAs have been well-studied. Multiple studies have revealed the critical role of miRNAs in various cardiovascular diseases, including cardiac hypertrophy, remodeling, arrhythmia, and heart failure.[28,29] Emerging evidence has also revealed the dysregulated expression of non-coding RNAs in multiple organs affected by IRI.[30–33] Based on the results of our previous studies, we focused on the expression levels of circRNA_0031672 and miR-21-5p in the pathogenesis of IRI. As expected, we observed dysregulated levels of circRNA_0031672 and miR-21-5p in both IRI rat models and H/R-treated cardiomyocytes.

The circRNA–miRNA–mRNA axis has been reported to play a vital role in mediating apoptosis during IRI. For example, the circDLGAP4/miR-143, circTLK1/miR-214/receptor-interacing protein kinase 1, and circNCX1/miR-133a-3p/cell death-inducing protein 1 pathways have been previously identified as potential regulators of cardiomyocyte apoptosis in myocardial IRI.[34–36] Another study showed that circDLGAP4 effectively restored the miR-143-repressed expression of homologous to E6-AP C-terminus domain E3 ubiquitin protein ligase 1, attenuating IRI-induced endothelial cell dysfunction by increasing cell viability and inhibiting apoptosis and migration.[37] Based on our results, the expression levels of circRNA_0031672, miR-21-5p, and PDCD4 were closely correlated with IRI. We identified a similar circRNA/miRNA regulatory machinery, where the circRNA_0031672/miR-21-5p/PDCD4 axis might prominently affect myocardial IRI by regulating H/R-induced apoptosis.

The most abundant type of RNA modification, m6A is highly enriched in the 3'UTR regions and is closely related to miRNAs in mRNA regulation.[16] In this study, we further evaluated the role of m6A modification in the 3'UTR of PDCD4 mRNA; however, m6A modifications did not influence the interaction between PDCD4 mRNA and miR-21-5p. Given that m6A modification did not prevent miR-21-5p from targeting the mRNA of PDCD4, we sought to target PDCD4 in cardiomyocytes by incubation with miR-21-5p-expressing BMSCs in subsequent experiments.

Even though pan-caspase inhibitors have been used to inhibit myocardial apoptosis in animal model, adverse side effects elicited by repressed mitochondrial function were prominent.[38,39] Therefore, the circRNA–miRNA–mRNA axis may offer better selectivity and could be a potential therapeutic target for IRI. Previous studies have indicated that miRNAs in exosomes secreted by BMSCs are crucial components regulating cardiovascular diseases as potential therapeutic tools.[40,41] Furthermore, BMSC-derived exosomes have been reported to induce proliferation and repress apoptosis in H9C2 cells.[42] In this study, we developed a miRNA delivery system by generating miR-21-5p-overexpressing BMSCs.

The genetically modified BMSCs may have secreted miR-21-5p-containing extracellular vesicles, which selectively enhanced the expression of miR-21-5p in H/R-treated cardiomyocytes. As a result, miR-21-5p expression in H/R-treated cardiomyocytes was restored by co-culture with miR-21-5p-overexpressing BMSCs. This strategy offers a potential therapeutic approach to prevent IRI-associated apoptosis, which is promising for application in the clinical setting for improving the prognosis of CHD patients. Our study in near future would transplant miR-21-5p-expressing BMSCs to identify the protective effect against IRI in cardiomyocytes in the animal model.

CONCLUSIONS

In this study, we transplanted miR-21-5p-expressing BMSCs to identify the protective effect against IRI in cardiomyocytes in an animal model. As a result, we uncovered a novel regulatory mechanism involving the circRNA_0031672/miR-21-5p/PDCD4 axis in apoptosis during I/R and developed miR-21-5p-expressing BMSCs for miR-21-5p delivery to block PDCD4-induced apoptosis during I/R.

ACKNOWLEDGMENTS

This study was supported by the Guangxi Natural Science Foundation (No.2018GXNSFAA294137 & No.2020GXNSFDA238007). All authors had no conflicts of interest to disclose.

REFERENCES

[1] Ren J, Zhang Y. New therapetic approaches in the management of ischemia reperfusion injury and cardiometabolic diseases: opportunities and challenges. *Curr Drug Targets* 2017; 18: 1687–1688.
[2] Chang X, Lochner A, Wang HH, *et al*. Coronary microvascular injury in myocardial infarction: perception and knowledge for mitochondrial quality control. *Theranostics* 2021; 11: 6766–6785.
[3] Wang J, Zhou H. Mitochondrial quality control mechanisms as molecular targets in cardiac ischemia-reperfusion injury. *Acta Pharm Sin B* 2020; 10: 1866–1879.
[4] Murphy E, Steenbergen C. Mechanisms underlying acute protection from cardiac ischemia-reperfusion injury. *Physiol Rev* 2008; 88: 581–609.
[5] Ma H, Guo R, Yu L, *et al*. Aldehyde dehydrogenase 2 (ALDH2) rescues myocardial ischaemia/reperfusion injury: role of autophagy paradox and toxic aldehyde. *Eur Heart J* 2011; 32: 1025–1038.
[6] Ye Y, Perez-Polo JR, Qian J, *et al*. The role of microRNA in modulating myocardial ischemia-reperfusion injury. *Physiol Genomics* 2011; 43: 534–542.
[7] Su S, Luo D, Liu X, *et al*. MiR-494 up-regulates the PI3K/Akt pathway via targetting PTEN and attenuates hepatic ischemia/reperfusion injury in a rat model. *Biosci Rep* 2017; 37: BSR20170798.
[8] Liu Z, Jiang J, Yang Q, *et al*. MicroRNA-682-mediated downregulation of PTEN in intestinal epithelial cells ameliorates intestinal ischemia-reperfusion injury. *Cell Death Dis* 2016; 7: e2210.
[9] Memczak S, Jens M, Elefsinioti A, *et al*. Circular RNAs are a large class of animal RNAs with regulatory potency. *Nature* 2013; 495: 333–338.
[10] Tay Y, Rinn J, Pandolfi PP. The multilayered complexity of ceRNA crosstalk and competition. *Nature* 2014; 505: 344–352.
[11] Zhong Z, Huang M, Lv M, *et al*. Circular RNA MYLK as a competing endogenous RNA promotes bladder cancer progression through modulating VEGFA/VEGFR2 signaling pathway. *Cancer Lett* 2017; 403: 305–317.
[12] Xue J, Chen C, Luo F, *et al*. CircLRP6 regulation of ZEB1 via miR-455 is involved in the epithelial-mesenchymal transition during arsenite-induced malignant transformation of human keratinocytes. *Toxicol Sci* 2018; 162: 450–461.
[13] Li J, Yang X, Qi Z, *et al*. The role of mRNA m6A methylation in the nervous system. *Cell Biosci* 2019; 9: 66.
[14] Wei CM, Gershowitz A, Moss B. Methylated nucleotides block 5′ terminus of HeLa cell messenger RNA. *Cell* 1975; 4: 379–386.
[15] Zhu ZM, Huo FC, Pei DS. Function and evolution of RNA N6-methyladenosine modification. *Int J Biol Sci* 2020; 16: 1929–1940.
[16] Meyer KD, Saletore Y, Zumbo P, *et al*. Comprehensive analysis of mRNA methylation reveals enrichment in 3′ UTRs and near stop codons. *Cell* 2012; 149: 1635–1646.
[17] Johnson J, Shojaee M, Mitchell Crow J, *et al*. From mesenchymal stromal cells to engineered extracellular vesicles: a new therapeutic paradigm. *Front Cell Dev Biol* 2021; 9: 705676.
[18] Guo Y, Yu Y, Hu S, *et al*. The therapeutic potential of mesenchymal stem cells for cardiovascular diseases. *Cell Death Dis* 2020; 11: 349.
[19] Zomer HD, Vidane AS, Gonçalves NN, *et al*. Mesenchymal and induced pluripotent stem cells: general insights and clinical perspectives. *Stem Cells Cloning* 2015; 8: 125–134.
[20] Gu H, Liu Z, Li Y, *et al*. Serum-derived extracellular vesicles protect against acute myocardial infarction by regulating miR-21/PDCD4 signaling pathway. *Front Physiol* 2018; 9: 348.
[21] Li S, Fan Q, He S, *et al*. MicroRNA-21 negatively regulates Treg cells through a TGF-beta1/Smad-independent pathway in patients with coronary heart disease. *Cell Physiol Biochem* 2015; 37: 866–878.
[22] Dong S, Cheng Y, Yang J, *et al*. MicroRNA expression signature and the role of microRNA-21 in the early phase of acute myocardial infarction. *J Biol Chem* 2009; 284: 29514–29525.
[23] Jia Z, Lian W, Shi H, *et al*. Ischemic postconditioning

protects against intestinal ischemia/reperfusion injury via the HIF-1alpha/miR-21 axis. *Sci Rep* 2017; 7: 16190.
[24] Shi H, Wang X, Lu Z, *et al*. YTHDF3 facilitates translation and decay of N6-methyladenosine-modified RNA. *Cell Res* 2017; 27: 315–328.
[25] Gilbert WV, Bell TA, Schaening C. Messenger RNA modifications: form, distribution, and function. *Science* 2016; 352: 1408–1412.
[26] Liu J, Yue Y, Han D, *et al*. A METTL3-METTL14 complex mediates mammalian nuclear RNA N6-adenosine methylation. *Nat Chem Biol* 2014; 10: 93–95.
[27] Li X, Wang X, Cheng Z, *et al*. AGO2 and its partners: a silencing complex, a chromatin modulator, and new features. *Crit Rev Biochem Mol Biol* 2020; 55: 33–53.
[28] Cao RY, Li Q, Miao Y, *et al*. The emerging role of microRNA-155 in cardiovascular diseases. *Biomed Res Int* 2016; 2016: 9869208.
[29] Gangwar RS, Rajagopalan S, Natarajan R, *et al*. Noncoding RNAs in cardiovascular disease: pathological relevance and emerging role as biomarkers and therapeutics. *Am J Hypertens* 2018; 31: 150–165.
[30] Lin L, Yang Z, Zheng G, *et al*. Analyses of changes in myocardial long non-coding RNA and mRNA profiles after severe hemorrhagic shock and resuscitation via RNA sequencing in a rat model. *BMC Mol Biol* 2018; 19: 11.
[31] Li H, Wu Y, Suo G, *et al*. Profiling neuron-autonomous lncRNA changes upon ischemia/reperfusion injury. *Biochem Biophys Res Commun* 2018; 495: 104–109.
[32] Zhou J, Chen H, Fan Y. Systematic analysis of the expression profile of non-coding RNAs involved in ischemia/reperfusion-induced acute kidney injury in mice using RNA sequencing. *Oncotarget* 2017; 8: 100196–100215.
[33] Chen Z, Luo Y, Yang W, *et al*. Comparison analysis of dysregulated lncRNA profile in mouse plasma and liver after hepatic ischemia/reperfusion injury. *PLoS One* 2015; 10: e0133462.
[34] Wang S, Chen J, Yu W, *et al*. Circular RNA DLGAP4 ameliorates cardiomyocyte apoptosis through regulating BCL2 via targeting miR-143 in myocardial ischemia-reperfusion injury. *Int J Cardiol* 2019; 279: 147.
[35] Song YF, Zhao L, Wang BC, *et al*. The circular RNA TLK1 exacerbates myocardial ischemia/reperfusion injury via targeting miR-214/RIPK1 through TNF signaling pathway. *Free Radic Biol Med* 2020; 155: 69–80.
[36] Li M, Ding W, Tariq MA, *et al*. A circular transcript of *ncx1* gene mediates ischemic myocardial injury by targeting miR-133a-3p. *Theranostics* 2018; 8: 5855–5869.
[37] Chen L, Luo W, Zhang W, *et al*. CircDLPAG4/HECTD1 mediates ischaemia/reperfusion injury in endothelial cells via ER stress. *RNA Biol* 2020; 17: 240–253.
[38] Holly TA, Drincic A, Byun Y, *et al*. Caspase inhibition reduces myocyte cell death induced by myocardial ischemia and reperfusion in vivo. *J Mol Cell Cardiol* 1999; 31: 1709–1715.
[39] Yaoita H, Ogawa K, Maehara K, *et al*. Attenuation of ischemia/reperfusion injury in rats by a caspase inhibitor. *Circulation* 1998; 97: 276–281.
[40] Xunian Z, Kalluri R. Biology and therapeutic potential of mesenchymal stem cell-derived exosomes. *Cancer Sci* 2020; 111: 3100–3110.
[41] Moghaddam AS, Afshari JT, Esmaeili SA, *et al*. Cardioprotective microRNAs: lessons from stem cell-derived exosomal microRNAs to treat cardiovascular disease. *Atherosclerosis* 2019; 285: 1–9.
[42] Shao L, Zhang Y, Lan B, *et al*. MiRNA-sequence indicates that mesenchymal stem cells and exosomes have similar mechanism to enhance cardiac repair. *Biomed Res Int* 2017; 2017: 4150705.

Please cite this article as: ZHANG J, LUO CJ, XIONG XQ, LI J, TANG SH, SUN L, SU Q. MiR-21-5p-expressing bone marrow mesenchymal stem cells alleviate myocardial ischemia/reperfusion injury by regulating the circRNA_0031672/miR-21-5p/programmed cell death protein 4 pathway. *J Geriatr Cardiol* 2021; 18(12): 1029–1043. DOI: 10.11909/j.issn.1671-5411.2021.12.004